Datasheet

VNIR Hyperspectral Camera | ATH1500

Feature:

- Spectral Range：400-1000nm
- Max Spatial Channels ：2048
- Max Spectral Channels ：1088
- Max FOV：51.7°(Depending on the lens)
- Superior imaging performance
- Data format is compatible with ENVI;
- Dimensions：132mm x 66mm x 65mm；
- Light weight：480g；
- No mechanical scanning, high reliability;

Application:

- Geological Survey Minerals;
- Agriculture Monitoring: Crops growth condition and yield assessment
- Forest pesticides and fire prevention monitoring；
- Coastline and ocean monitoring；
- Pasture monitoring；
- Lake and watershed monitoring；
- Remote sensing teaching and research ；
- Industrial sorting；
- Ecological environment protection in mining areas；
- Water quality and soil monitoring；
- Agriculture & Livestock Products Quality Monitoring
- Military, Defense & Homeland Safety；
- Geological Disaster Prevention

Describe:

ATH1500 is newly designed optimized VNIR imager camera, the breakthrough compact size, light weight, working wavelength range 400-1000nm, especially fit to airborne. Besides size and weight advantages, it employs high spatial resolution, and spectral resolution, wide imaging range. ATH1500 consists of two parts, imaging lens and hyperspectral imager.

ATH1500 employs 2048*1088pixels high performance CCD imaging components, clear imaging, low noise and good linearity.

ATH1500 depends on perfect optical system design with high temperature stability, it provides excellent stability and sensitivity required by VNIR chemical imaging application industries. It can satisfy strict requirements in the lab, field, industrial application , and it can ensure good quality of the pharmaceutical drugs, food safety and agriculture analysis.

Floor 22th, Creative Bld., 1300 Jimei Ave, Jimei, Xiamen, 361005, China
Tel: +86-592-6102588

1. Performance Parameter

ITEM	PARAMETER
Spectral Range	400-1000nm
Spectral Resolution	<10nm
Max. Spectral Channels	1088
Max. Spatial Channels	2048
Detector	High Sensitivity VNIR detector
Detector Interface	3.0
Detector Power Supply	12V±10%，6-10W
Raw resolution of detector	2048 X 1088
Raw pixels of detector	5.5 μm x 5.5 μm
Bit Depth	12 bits
FOV	15.2°@f=35mm (Depends on lens)
IFOV	0.7mrad@f=35mm 0.7mrad@f=35mm (Depends on lens)
Max. Frame Rate	240 fps
Dimension	132mm x66mm x 65mm
Weight	<480g
Working Temp.	-20 - 50°C
Storage Temp.	-30-70°C

Floor 22th, Creative Bld., 1300 Jimei Ave, Jimei, Xiamen, 361005, China
Tel: +86-592-6102588

2. ATH1500 Images Quality

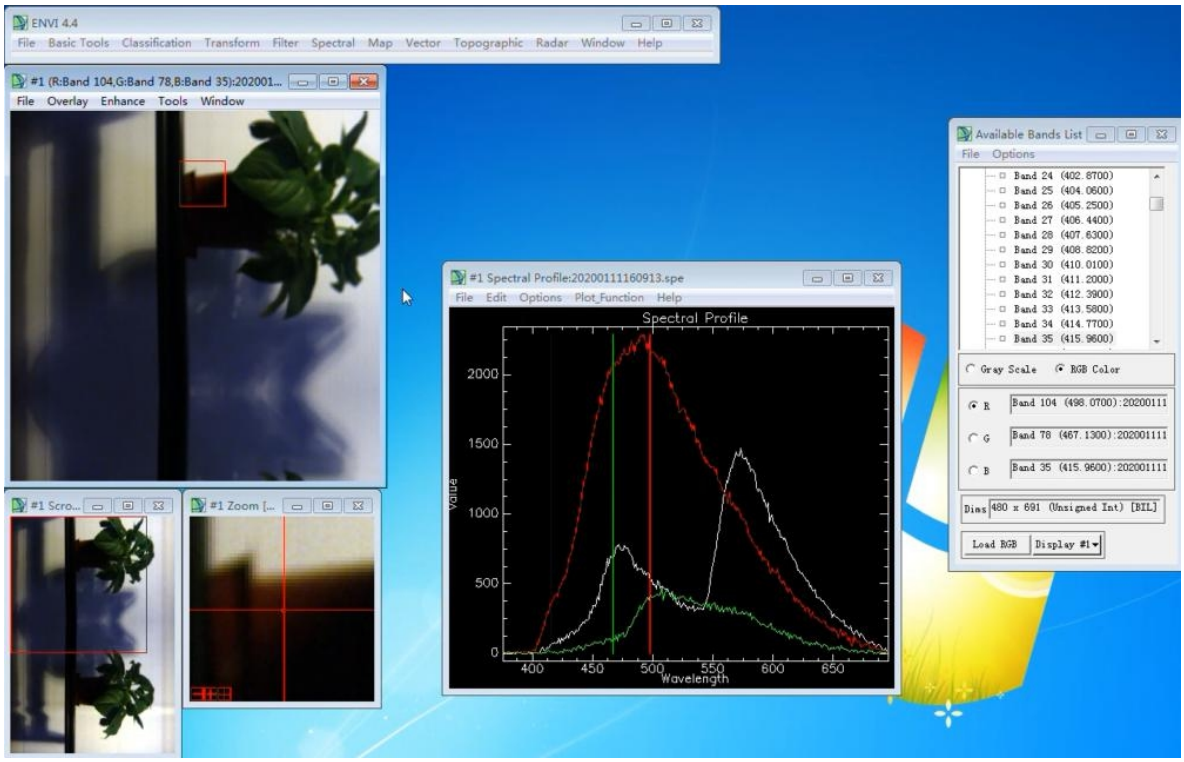

Fig 1 ATH1500 scan hyperspectral database

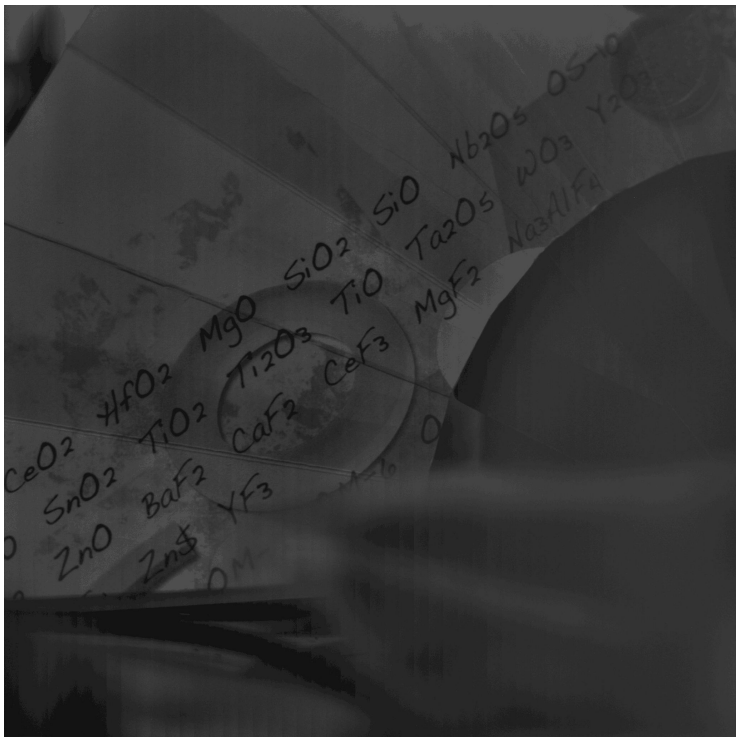

Fig 2 ATH1500 scan the 493nm band image

Floor 22th, Creative Bld., 1300 Jimei Ave, Jimei, Xiamen, 361005, China
Tel: +86-592-6102588

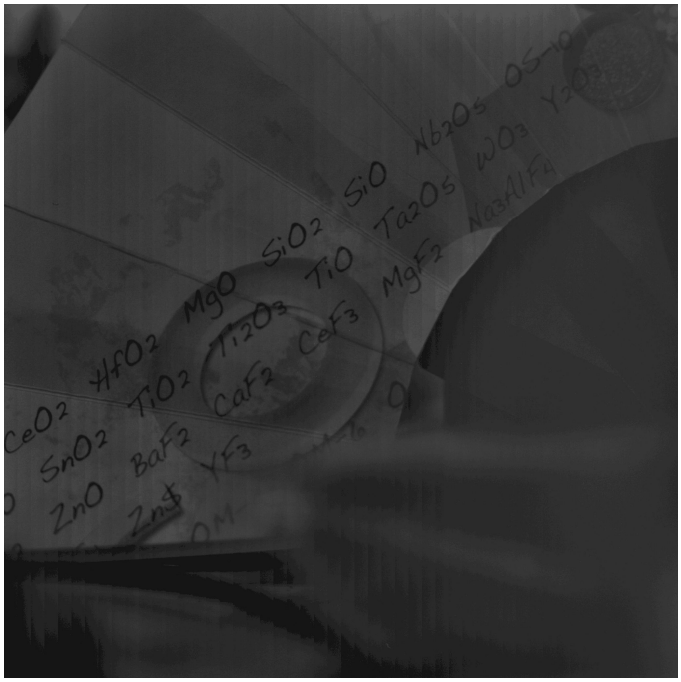

Fig 3 ATH1500 scan the 653nm band image

3. ATH1500 Hyperspectral Camera Series

ATH1500 Models	Feature	Application
ATH1500	400-1000nm VIS-NIR Hyperspectral Camera	a, Agriculture & Forestry: precision farming, pests and diseases, vegetation analysis, planting area evaluation, crop yield evaluation, b, Environmental Industry: water quality analysis, oil pollution monitoring c, Industrial sorting: fruit sorting, d, Archaeology: artwork scanning, cultural relic identification, pattern scanning
ATH1500-17	1.0~1.7μm SWIR Hyperspectral Camera	a, Semiconductor,Industrial sorting, food sorting, construction waste sorting, meat sorting, plastic sorting c, Geological survey, mineral survey d, Cultural relic identification, judicial identification, document inspection
ATH1500-25	1.2~2.5μm SWIR Hyperspectral Camera	a, precision agriculture and food analysis, moisture content analysis b, dark plastic sorting, medicine and material sorting,waste recycling c, geological survey, mineral survey, national defense and military industry, mineral mapping c, cultural relic identification, d, judicial identification, document inspection, medical identification
ATH1500-50	2.5~5.0μm MWIR Hyperspectral Camera	Geological survey, mineral sorting,land cover type identification

Floor 22th, Creative Bld., 1300 Jimei Ave, Jimei, Xiamen, 361005, China
Tel: +86-592-6102588

		national defense and military industry, camouflage investigation gas analysis, VOCs inspection water temperature detection
ATH1500-12-50	1.2~5.0μm SWIR Hyperspectral Camera	Geological survey national defense and military industry, camouflage investigation gas analysis, VOCs inspection, water temperature detection, land cover type identification, mineral sorting
ATH1500-04-17	0.4~1.7μm VIS-NIR Hyperspectral Camera	Precision agriculture, agricultural and forestry pests and diseases, vegetation analysis, planting area evaluation, crop yield evaluation, water quality analysis, oil pollution detection artwork scanning, cultural relic identification, pattern scanning, industrial sorting

4. Application

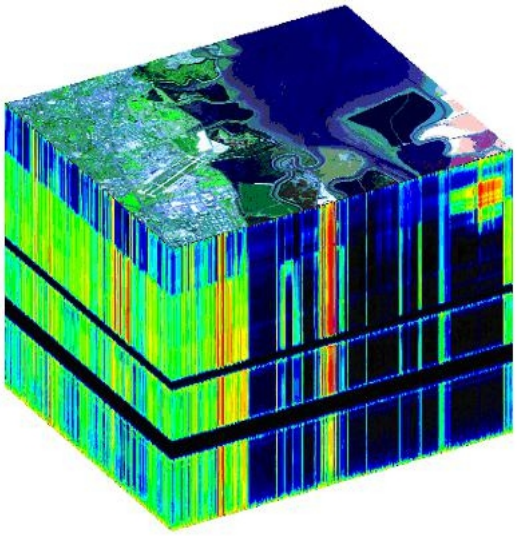

Figure 2 Data cube captured

Figure 3 Drone experiment

Floor 22th, Creative Bld., 1300 Jimei Ave, Jimei, Xiamen, 361005, China
Tel: +86-592-6102588

Figure 4 Outdoor experiment sceneI

Figure 5 Outdoor experiment sceneII

Floor 22th, Creative Bld., 1300 Jimei Ave, Jimei, Xiamen, 361005, China
Tel: +86-592-6102588

Figure 6 Outdoor experiment scene III

Floor 22th, Creative Bld., 1300 Jimei Ave, Jimei, Xiamen, 361005, China
Tel: +86-592-6102588

Figure 7 Outdoor experiment scene IV

Figure 8 Outdoor experiment sceneV

Floor 22th, Creative Bld., 1300 Jimei Ave, Jimei, Xiamen, 361005, China
Tel: +86-592-6102588

4.1 Industrial Sorting Application

With the development of NIR hyperspectral technology, such as Jiang tried to use near-infrared hyperspectral technology to detect impurities in cotton, especially the application of SWIR hyperspectral technology, which significantly improved the detection rate of plastic films compared with conventional methods.

Hyperspectral imaging technology is based on a very large number of narrow-band image data technology, which can obtain image information and spectral information of the sample while imaging the sample. Commonly used hyperspectral data processing methods include partial least squares (PLS), support vector machine (SVM) and artificial neural network (ANN).

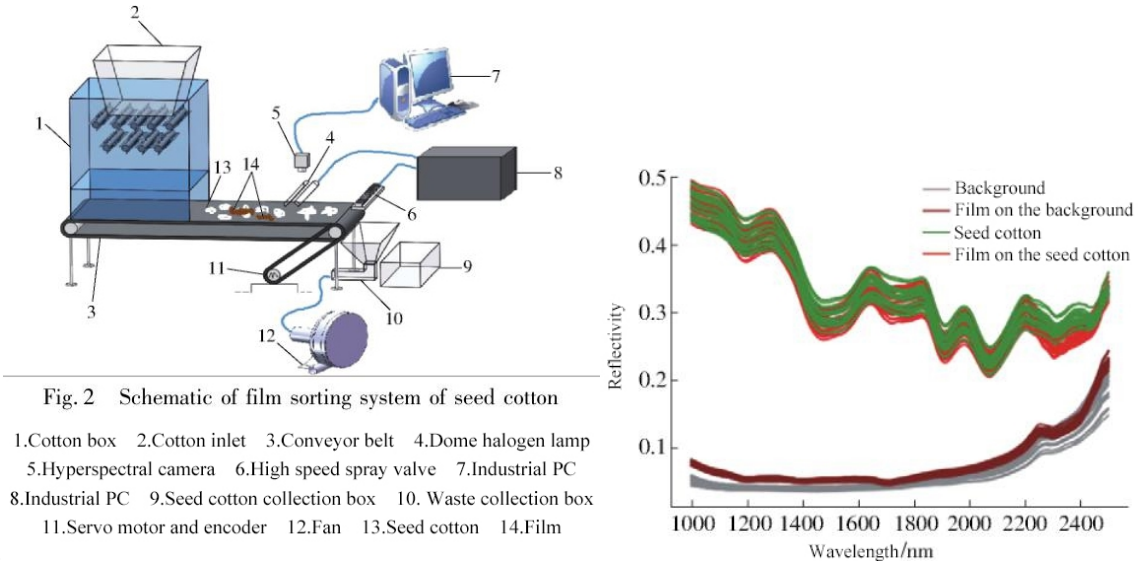

Fig. 2 Schematic of film sorting system of seed cotton

1.Cotton box 2.Cotton inlet 3.Conveyor belt 4.Dome halogen lamp 5.Hyperspectral camera 6.High speed spray valve 7.Industrial PC 8.Industrial PC 9.Seed cotton collection box 10. Waste collection box 11.Servo motor and encoder 12.Fan 13.Seed cotton 14.Film

.

Figure 9 Seed cotton sorting application; (a) System functional composition; (b) Different substances reflectance spectrum

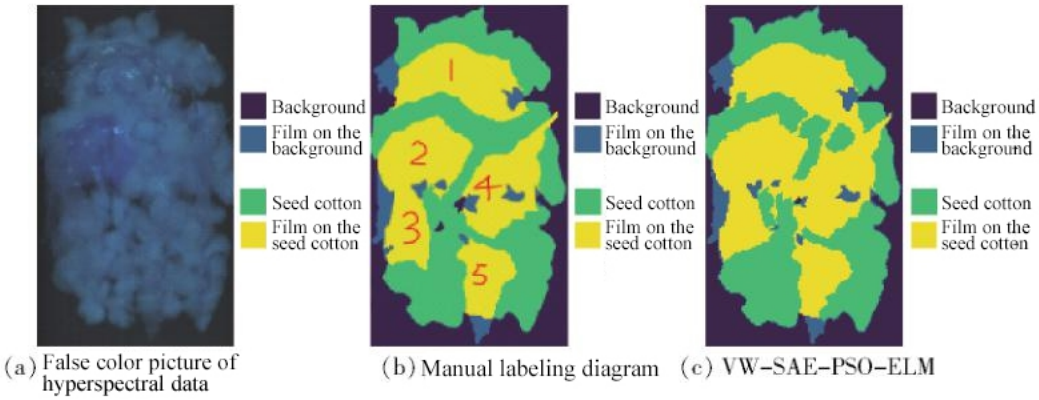

Figure 10 Seed cotton sorting application; (a) Artificial marking; (b) Recognition result

Apple's external quality is the most intuitive quality feature of Apple, which directly affects Apple's price and consumer preference. Aiming at the difficulties and key points of external inspection of apples, based on machine vision technology, hyperspectral imaging technology and multispectral imaging technology, integrated image processing technology, pattern recognition method, chemometric method and spectral analysis technology, the external physical quality of apple (shape and size) and detection

Floor 22th, Creative Bld., 1300 Jimei Ave, Jimei, Xiamen, 361005, China
Tel: +86-592-6102588

methods for common defects on the surface.

The detection system and algorithm developed on the basis of the above research laid the foundation for my country's research and development of rapid online inspection and grading equipment for Apple's external quality based on machine vision technology and multi-spectral machine vision technology.

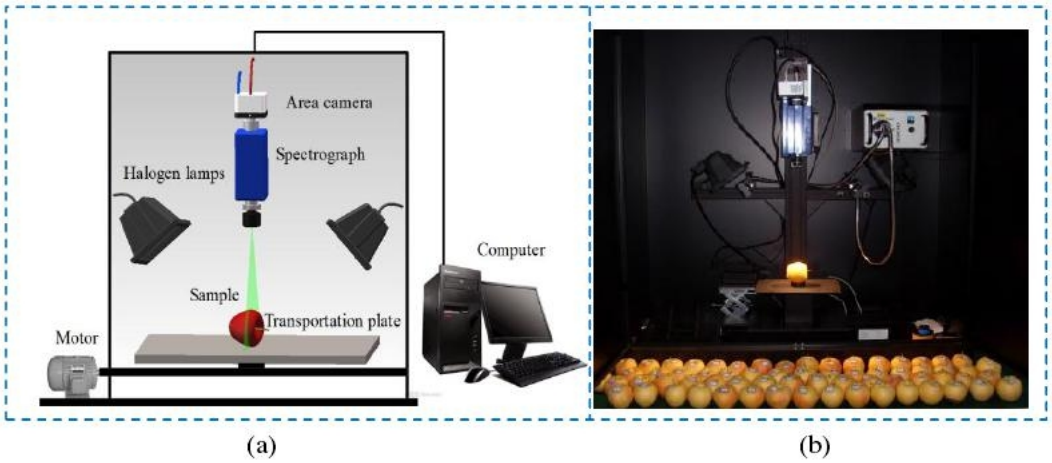

Figure 11 Schematic diagram and physical diagram developed by Dr. Zhang Baohua of Shanghai Jiaotong University; (a) Schematic diagram; (b) Physical diagram

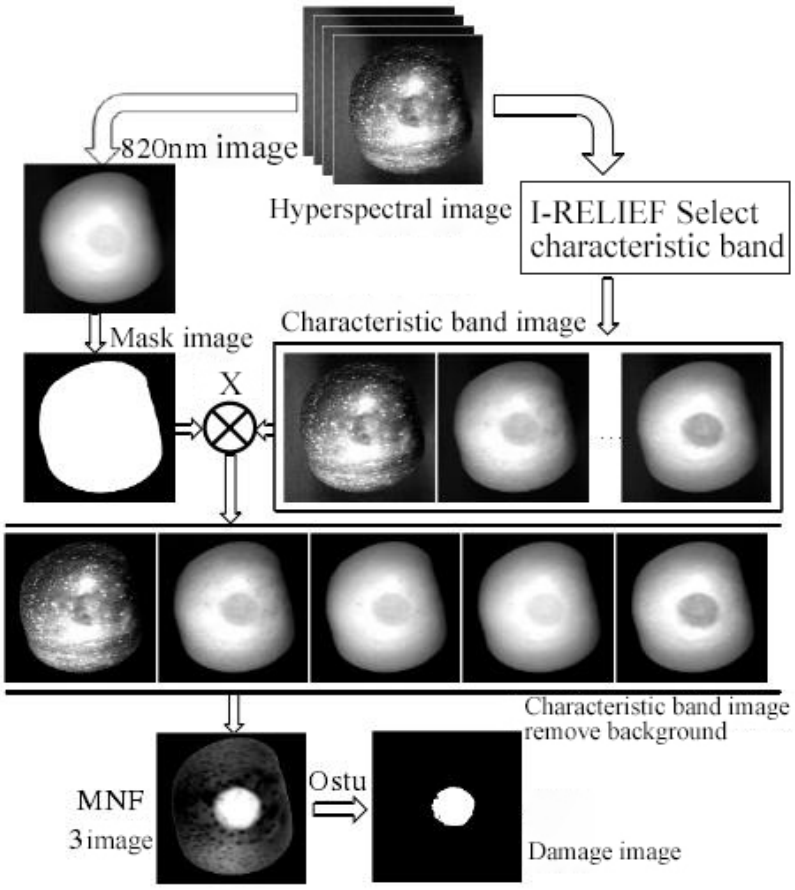

Figure 12: Flow chart of early damage detection algorithm for apple surface

Floor 22th, Creative Bld., 1300 Jimei Ave, Jimei, Xiamen, 361005, China
Tel: +86-592-6102588

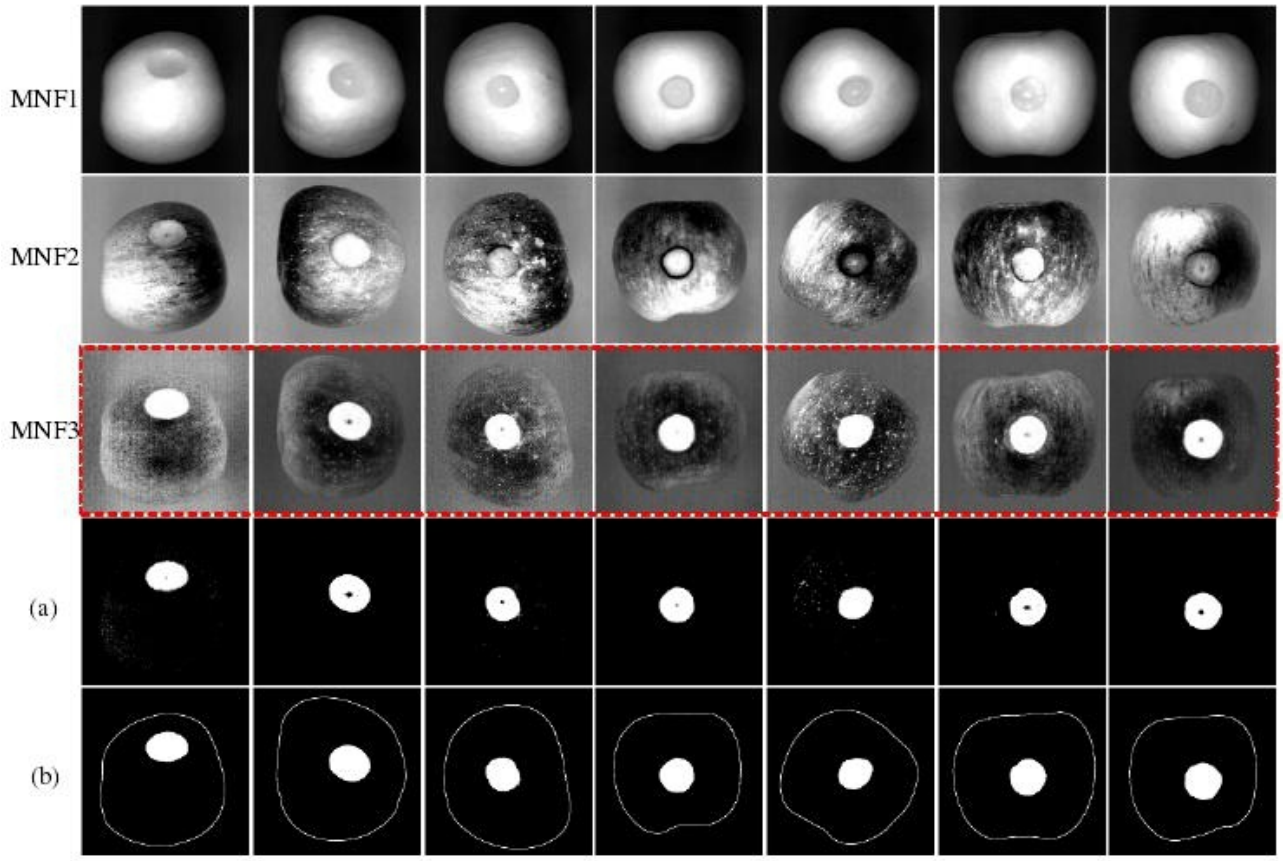

Figure 13 Recognition results of early decay of some apples and intermediate processing (a) rot segmentation results (b) final results

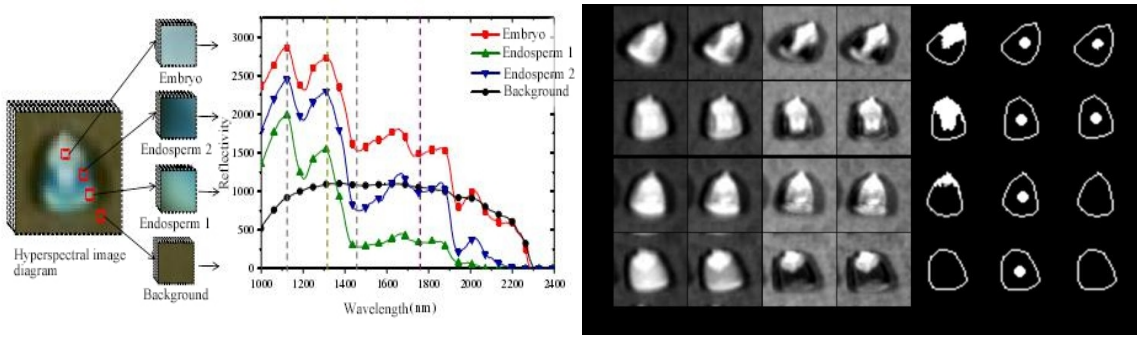

Figure 14 Corn seed sorting application (Dr. Chaopeng Wang, Northwest A&F University)

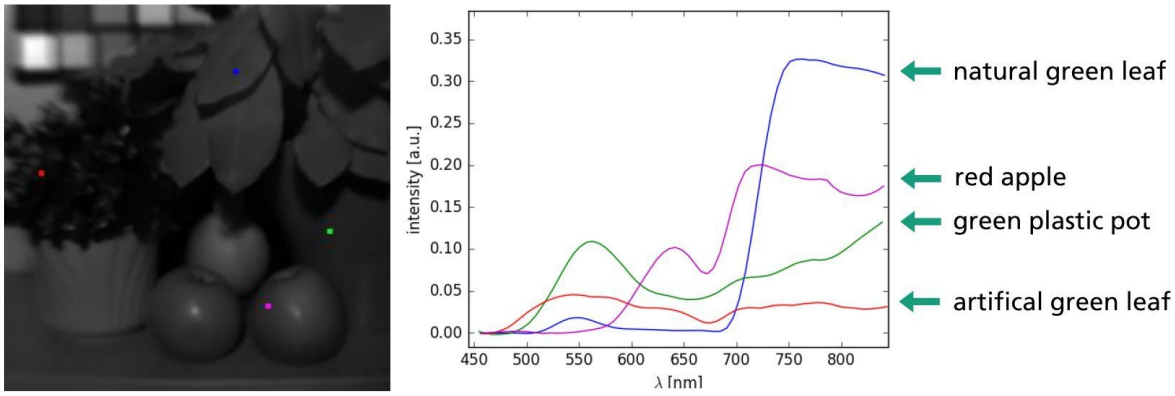

Floor 22th, Creative Bld., 1300 Jimei Ave, Jimei, Xiamen, 361005, China
Tel: +86-592-6102588

Figure 15 The spectrum of natural green plants, artificial green leaves, green plastic, and red apples

4.2 Precision Agriculture Application

Figure 16 Drone-borne hyperspectral imaging camera

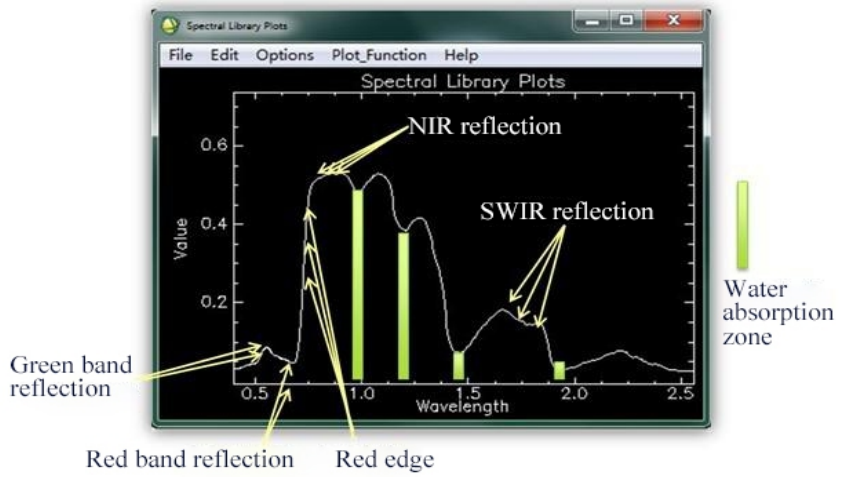

Figure 17 Green plants measured spectrum

1) **Crop growth monitoring and yield estimation:** Due to the different external factors of crops at each stage of their growth and development, there will be certain differences in their internal composition and external morphology. The most important difference is the leaf area index. Leaf area index is a comprehensive index reflecting the individual characteristics and group characteristics of crops.
2) **Crop pest control:** Remote sensing technology can monitor the effects of pests and diseases on the growth and development of crops, track the growth and development of crops, analyze and estimate disaster losses, and can monitor the distribution and activity of pests, thereby preventing the occurrence of pests.
3) **Drought monitoring of crops:** Remote sensing technology monitors crop drought conditions

Floor 22th, Creative Bld., 1300 Jimei Ave, Jimei, Xiamen, 361005, China
Tel: +86-592-6102588

through crop vegetation index and canopy parameters.

4) **Monitoring of soil moisture content and distribution:** In the case of different thermal inertia conditions, the difference between remote sensing spectra is very obvious, so a mathematical model between thermal inertia and soil moisture content can be established, and remote sensing technology uses this model to analyze soil moisture content and distribution.

5) **Crop nutrient monitoring:** The accuracy of remote sensing technology to monitor the nitrogen content of crops is higher than that of other nutrient elements.

Normalized difference spectral index (NDSI), ratio spectral index (RSI) and simple spectral index (SSI) were constructed by using single band and any two bands in the range of 450 ~ 882 nm to calculate the correlation between CGI and spectral index and screen out spectral index with good correlation. Combined with partial least squares regression (PLSR), the inversion model was established.

Using CGI as the index, Airborne hyperspectral image was used to monitor the growth status of wheat in the multi-growth period in 2015. Unmanned aerial vehicle hyperspectral image inversion CGI has high precision, which can judge the difference of wheat overall growth, and can provide reference for wheat growth monitoring.

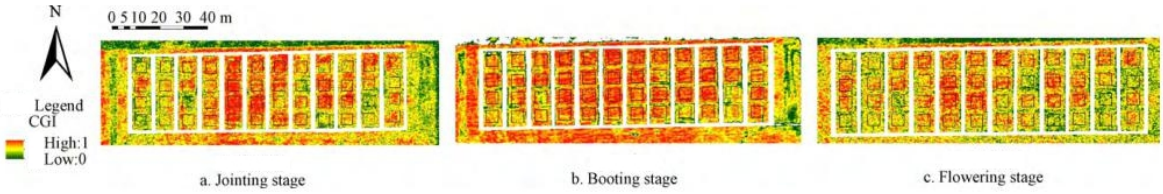

Figure 18 CGI inversion of wheat growth index

4.3 Forest Health Application

Used for pest monitoring and forest resource assessment.

Principle: The health of vegetation is related to greenness index, leaf area index, leaf moisture content and light use efficiency;

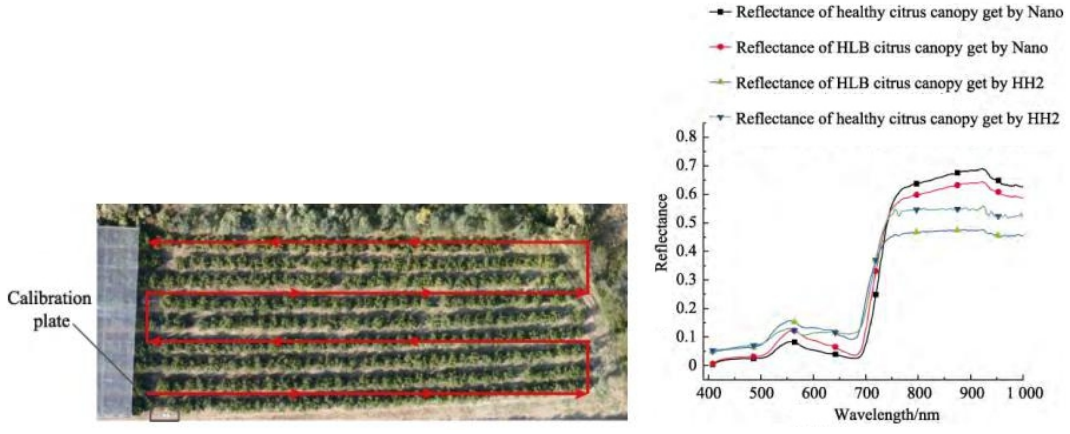

Figure 19 Monitoring and classification of citrus yellow dragon disease plants based on drone-borne hyperspectral imaging camera (designed by Lan Yubin et al., South China Agricultural University)

Floor 22th, Creative Bld., 1300 Jimei Ave, Jimei, Xiamen, 361005, China
Tel: +86-592-6102588

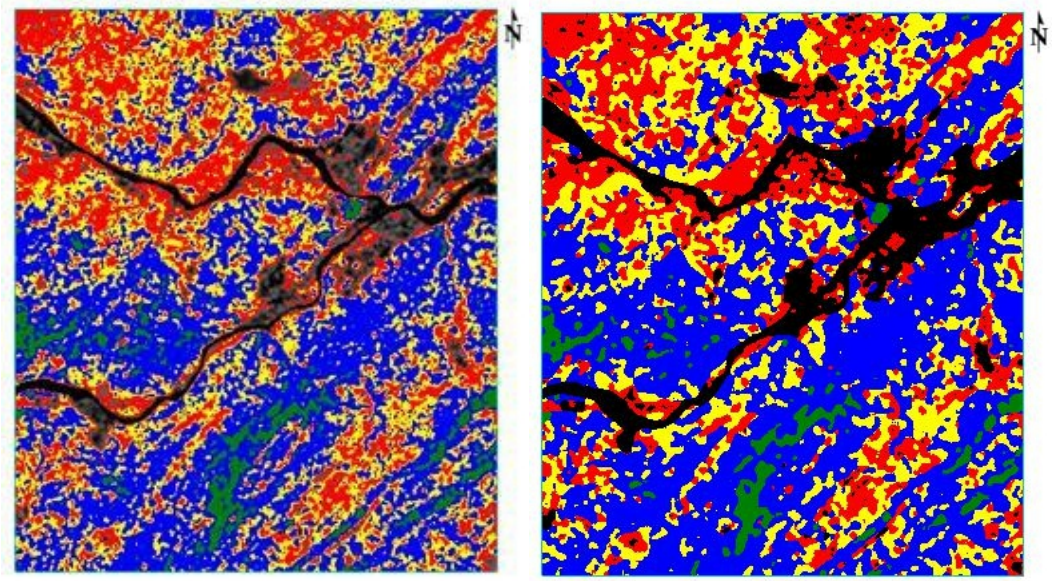

Figure 20 Distribution map of masson pine health degree studied by Wang Shuang of the University of Electronic Science and Technology of China with a hyperspectral camera

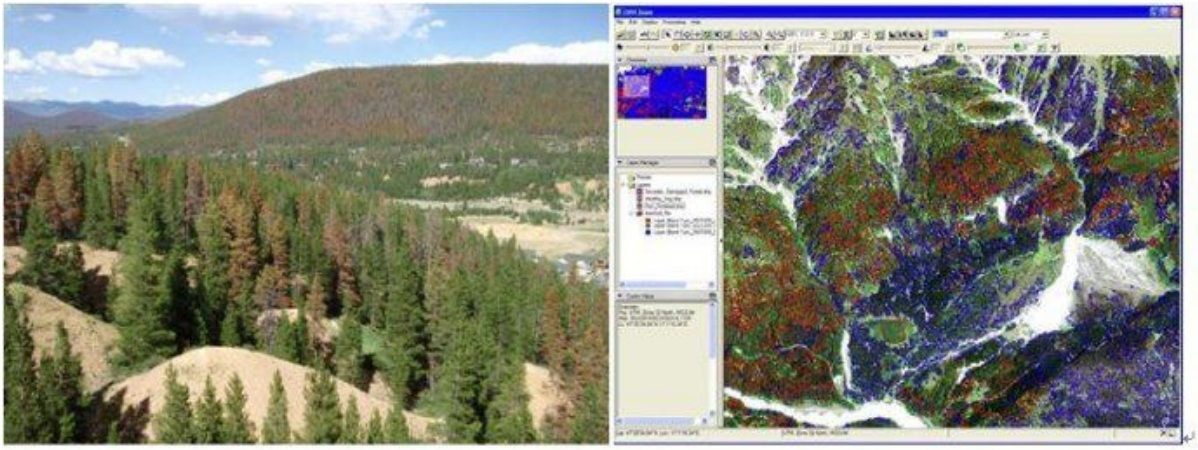

4.4 Geological Survey Application

Spectral remote sensing technology evolved from the multi-spectral remote sensing technology represented by Landsat and took initial shape in the mid-1980s (Goets et al., 1985, Tong Qingxi et al., 2006).

Due to its advantages of high spectral resolution and atlas integration, hyperspectral remote sensing technology has the ability of fine detection and analysis of surface rock mineral composition on a large scale. It can not only provide a macro image of the ground, but also determine the type and abundance of minerals in the geological body, and even the chemical composition of some minerals at pixel level details (Wang Runsheng et al., 2010).

In recent years, with the continuous development of hardware, data processing methods and software related to imaging spectrometer, the application of hyperspectral remote sensing technology in the field of geological survey has been accelerated.

Hyperspectral remote sensing technology has played an important role in geological mapping, the

Floor 22th, Creative Bld., 1300 Jimei Ave, Jimei, Xiamen, 361005, China
Tel: +86-592-6102588

definition and division of hydrothermal alteration zones, and the delineation and discrimination of mineralization anomalies from large metallogenic areas to medium-scale ore fields (e.g. Bierwirth et al., 2002; Company Changyun et al., 2005; Kruse et al., 2006; Cudahy et al., 2007; Wang Runsheng et al., 2010; Liu Dechang et al., 2011; Yan Baikun et al., 2014; Yang Zian et al., 2015; Graham et al., 2017).

With the theory of metallogenic system (Wyborn et al., 1994) becoming the guiding principle of prospecting practice, thematic mineral mapping on the scale of large ore concentration areas and metallogenic belts will provide key regional material composition information for predictive prospecting and exploration.

The spectral wavelength ranges used for mineral mapping include visible light (400-700nm), NIR (700-1000nm), SWIR (1000-2500nm), and thermal IR (7000-15000nm). At present, the most widely used in mining is the short-wave infrared region (1000-2500nm).

Because the frequency is close to the cofrequency and combined frequency of the chemical bond vibration in the mineral lattice, the mineral containing water or OH- (mainly layered silicate and clay) as well as some sulfate and carbonate minerals can be observed in the range of short-wave infrared wavelength.

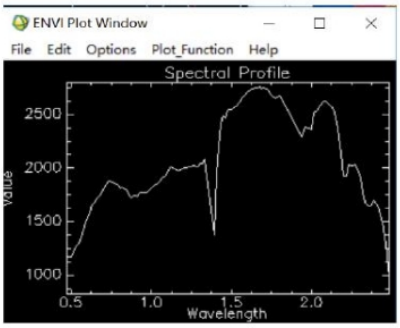

HH036 point image spectrum

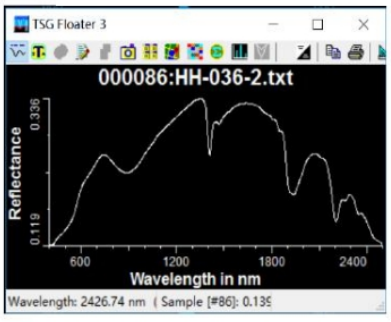

HH036 point measurede spectrum

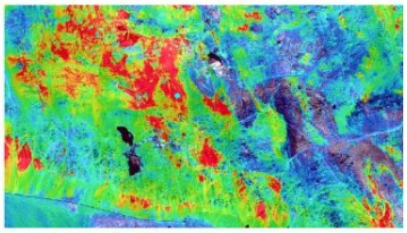

Sericite Filling Results Comparison of known deposit points between HH036 and measured

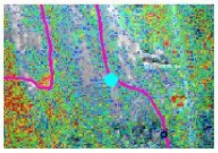

Chlorite extraction results

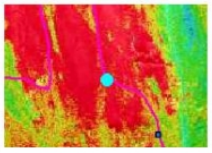

Sericite extraction results

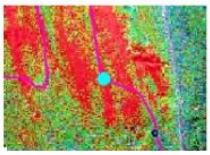

Feb3+ extraction result

Sampling point photos

Long-range photos of sampling points

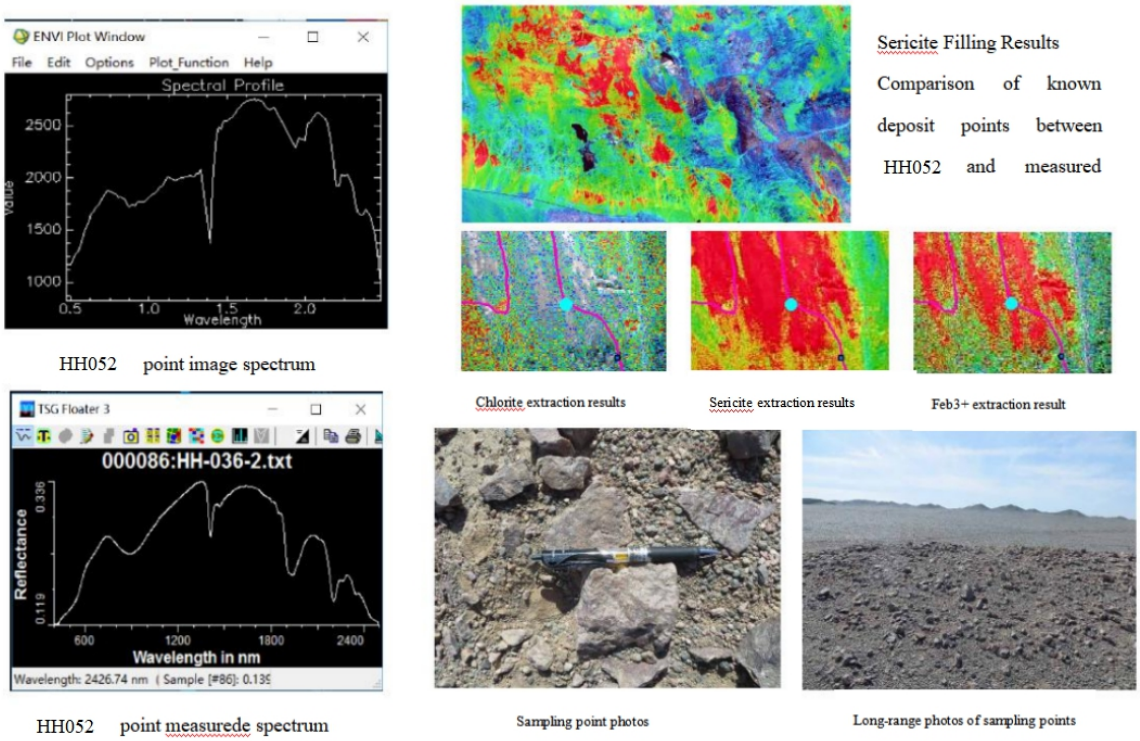

Figure 21 Application of hyperspectral imager in prospecting

Soil salinization is one of the important ecological and environmental problems in arid and semi-arid areas. Soil salinization causes soil hardening, fertility decline, acid-base imbalance, land degradation and other consequences, which seriously restricts agricultural development in China and affects the strategic situation of sustainable development in China at present.Remote sensing technology, with its characteristics of large scale, wide range, strong timeliness and economy, makes up for the deficiency of traditional methods for monitoring salinization phenomenon, and provides a new way for quantitative monitoring of soil salinization phenomenon.

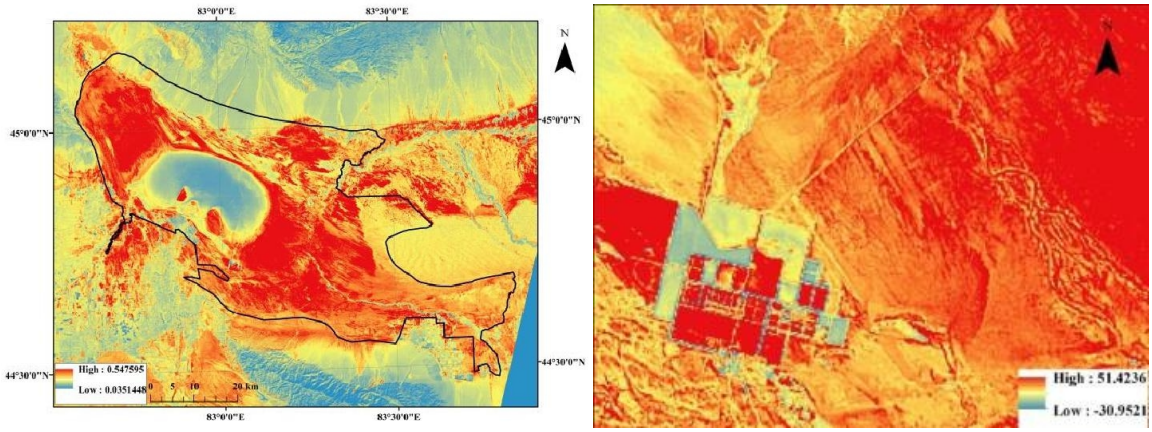

Figure 22 The surrounding area of a salt field

Floor 22th, Creative Bld., 1300 Jimei Ave, Jimei, Xiamen, 361005, China
Tel: +86-592-6102588

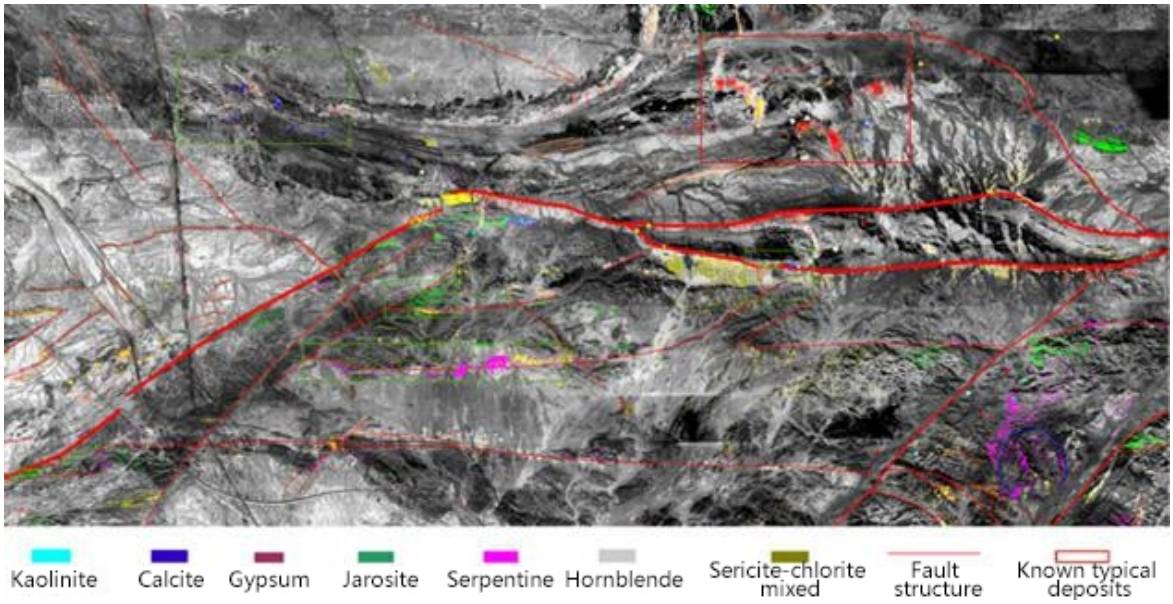

4.5 Public Safety Application

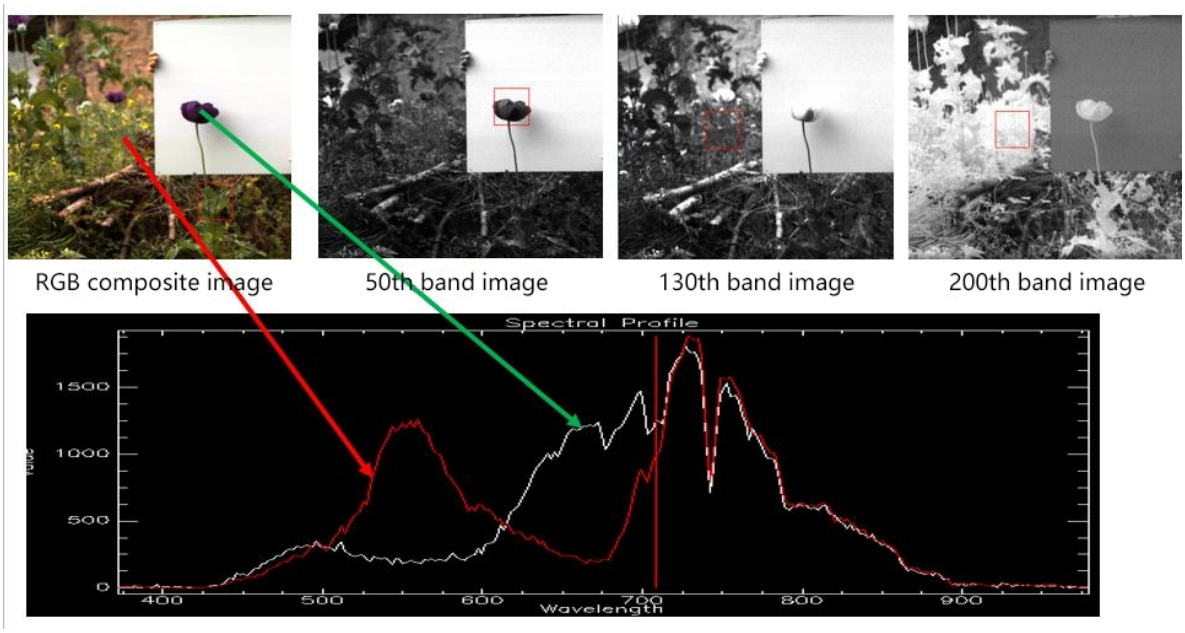

Figure 23 The searching for illegal poppy cultivation application

Figure 24 Document inspection application

Floor 22th, Creative Bld., 1300 Jimei Ave, Jimei, Xiamen, 361005, China
Tel: +86-592-6102588

4.6 Medical Microscopic Imaging Application

Objective: online detection and navigation positioning during tumor surgery

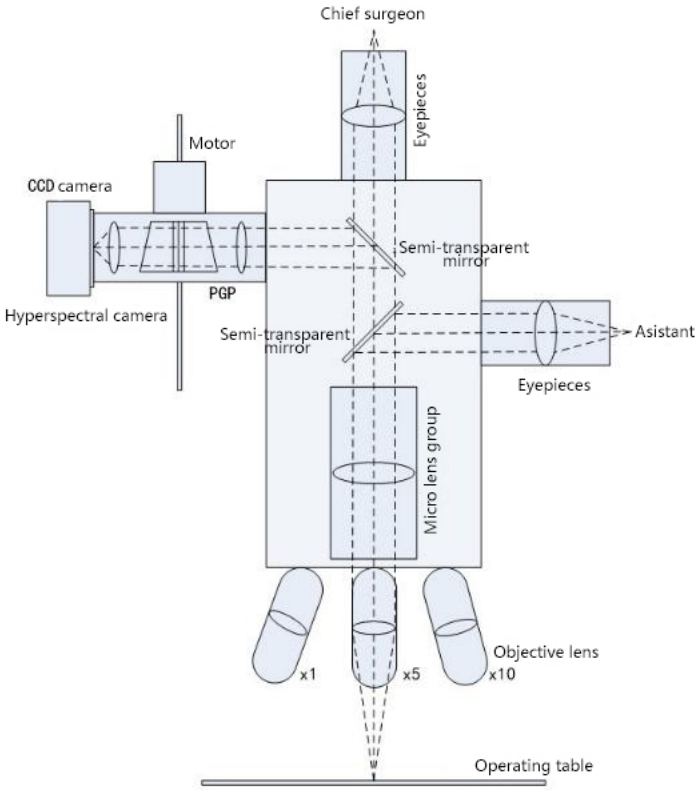

Figure 25 Medical microscope imager optical path schematic diagram

Is shown in the figure of medical microscopic imaging spectrometer principle diagram, the operating table for the target after the objective lens, microscope lens group is divided into three road, visual observation for the surgeon, all the way all the way for the assistant auxiliary visual observation, a routing imaging spectrometer detection, driven by a motor to imaging spectrometer measuring target space d scanning, imaging spectral information of the target under test, then through data analysis, image processing, through the display to the doctor.

Floor 22th, Creative Bld., 1300 Jimei Ave, Jimei, Xiamen, 361005, China
Tel: +86-592-6102588

Figure 26 Medical microscope imager figure

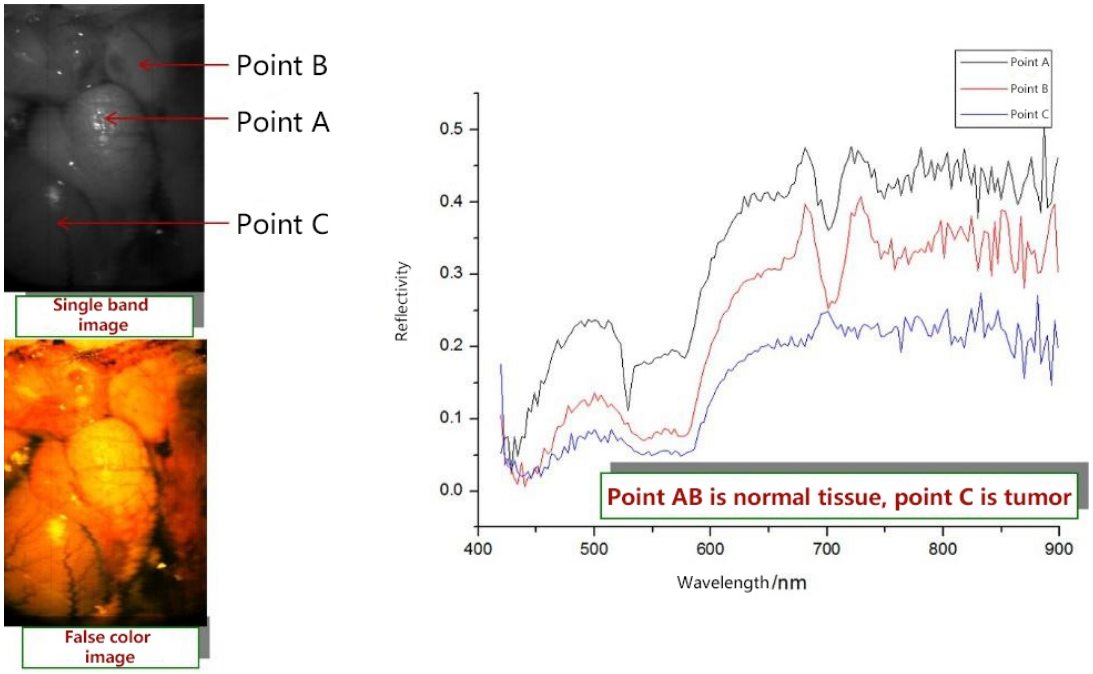

Figure 27 Data collect by medical microscopic imager

4.7 Airborne Hyperspectral Imaging System Application

Floor 22th, Creative Bld., 1300 Jimei Ave, Jimei, Xiamen, 361005, China
Tel: +86-592-6102588

Figure 28 Optosky Airborne Imaging Camera

Objective: Airborne remote sensing

Application: Figure shows airborne imager consists of SpecVIEW-VIS, stable platform and POS modules. Figure 30 and Figure 31 show data was collected. Figure 7 shows pseudo color image processed through geometric correction, flight strip spice and radiatation correction. Figure 31 shows typical geology spectral curve.

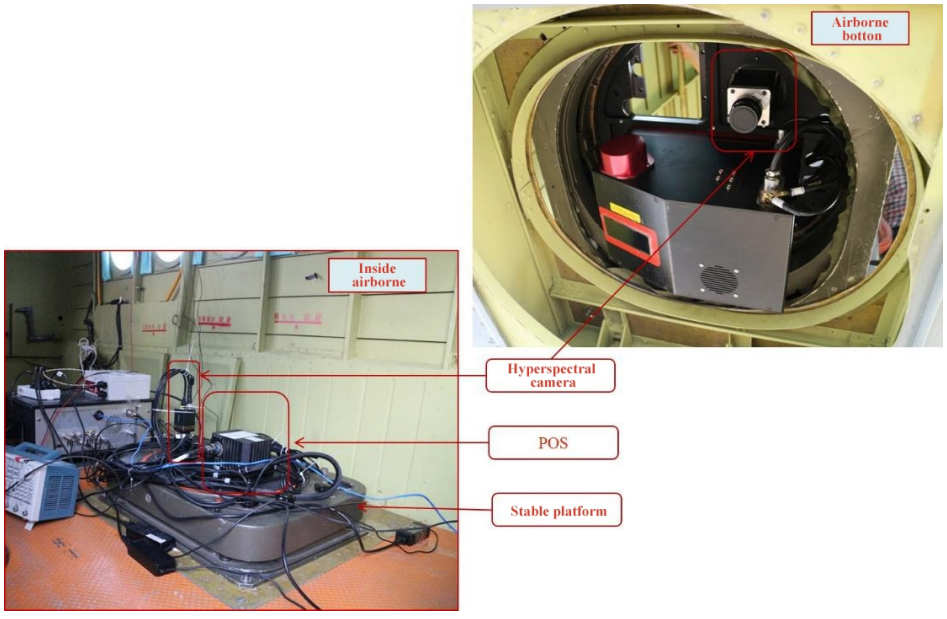

Floor 22th, Creative Bld., 1300 Jimei Ave, Jimei, Xiamen, 361005, China
Tel: +86-592-6102588

Figure 29 Airborne remote sensing application

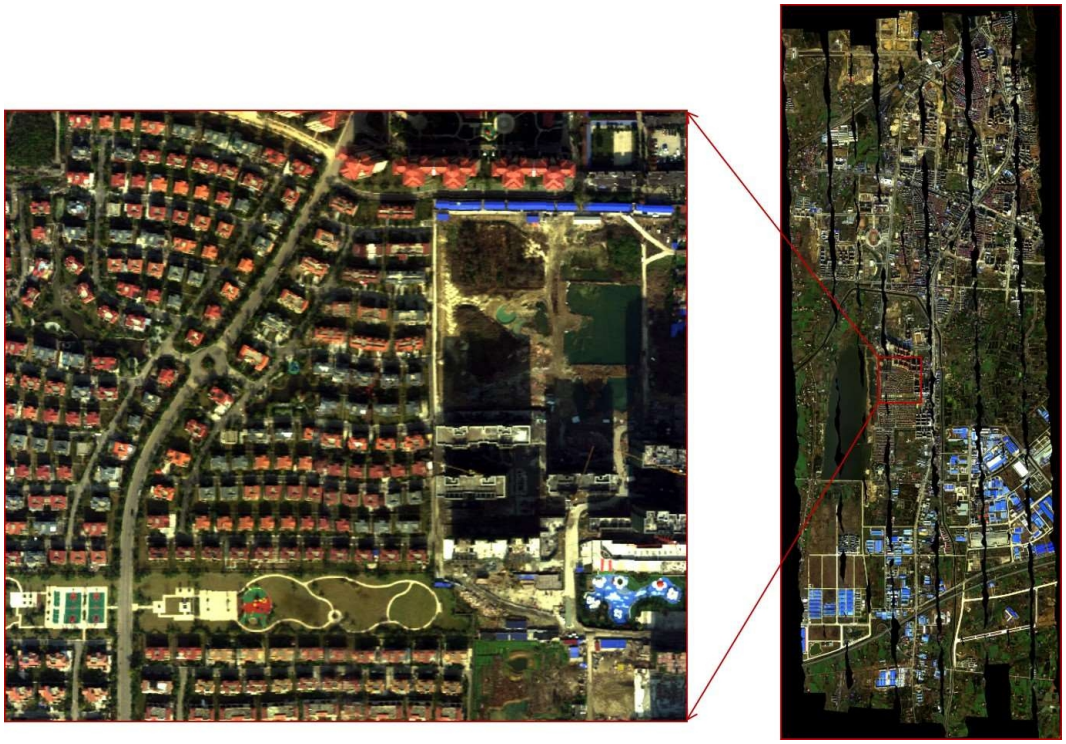

Figure 30 Airborne application data-pseudocolor image

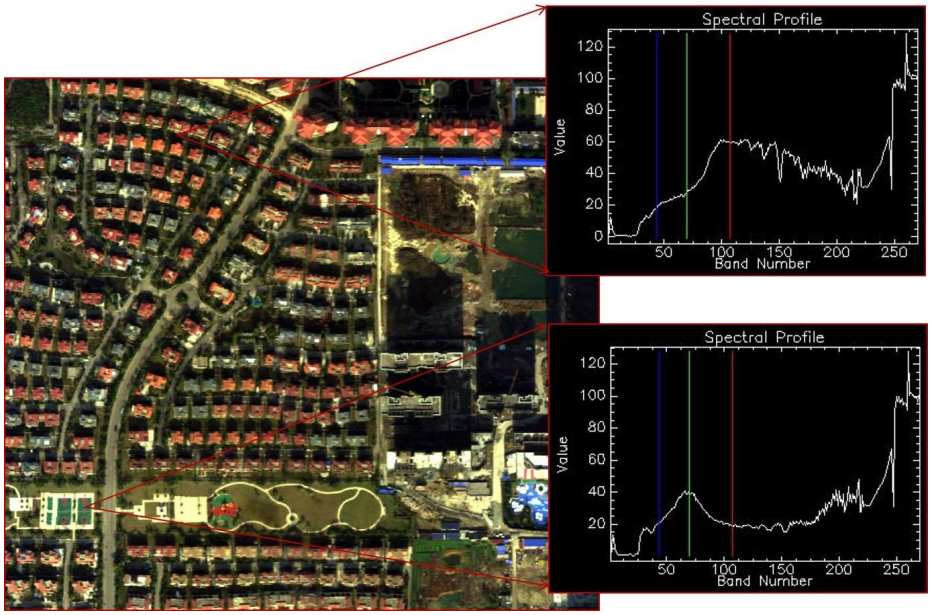

Figure 31 Airborne application data-spectral curve

Floor 22th, Creative Bld., 1300 Jimei Ave, Jimei, Xiamen, 361005, China
Tel: +86-592-6102588

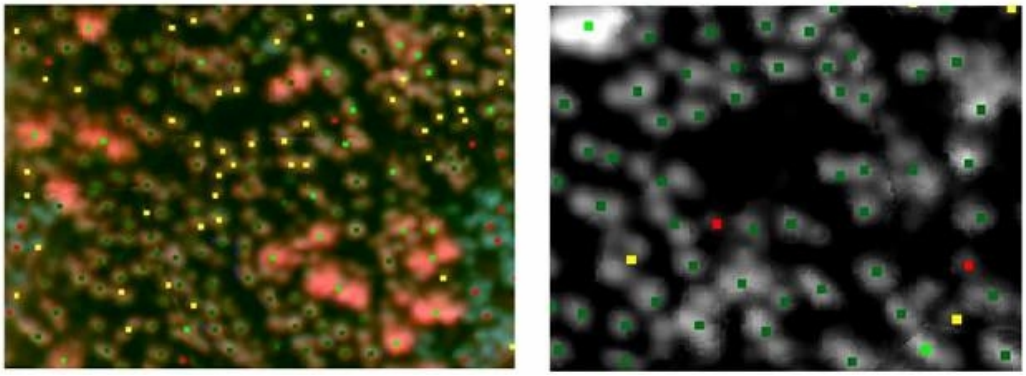

Figure 32 Forest remote sensing, Airborne hyperspectral monitor forest disease and pest

4.8 Water Quality and Environmental Protection Application

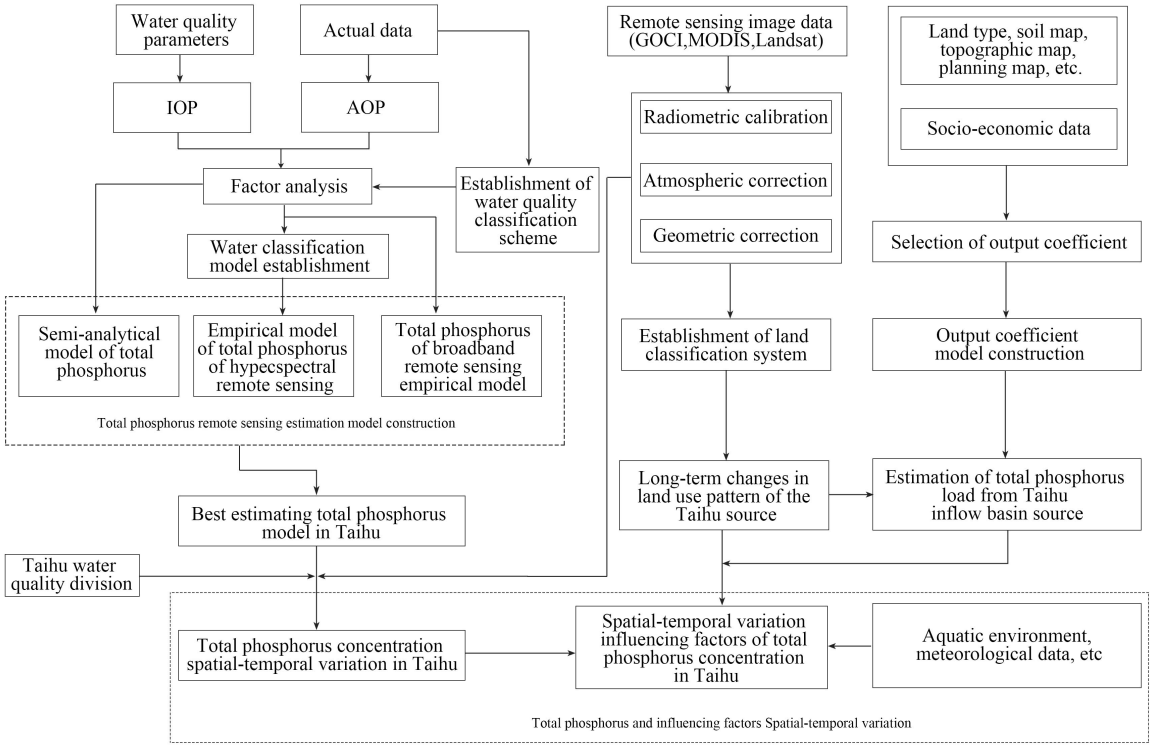

Figure 33 Inversion algorithm flow of hyperspectral data

Floor 22th, Creative Bld., 1300 Jimei Ave, Jimei, Xiamen, 361005, China
Tel: +86-592-6102588

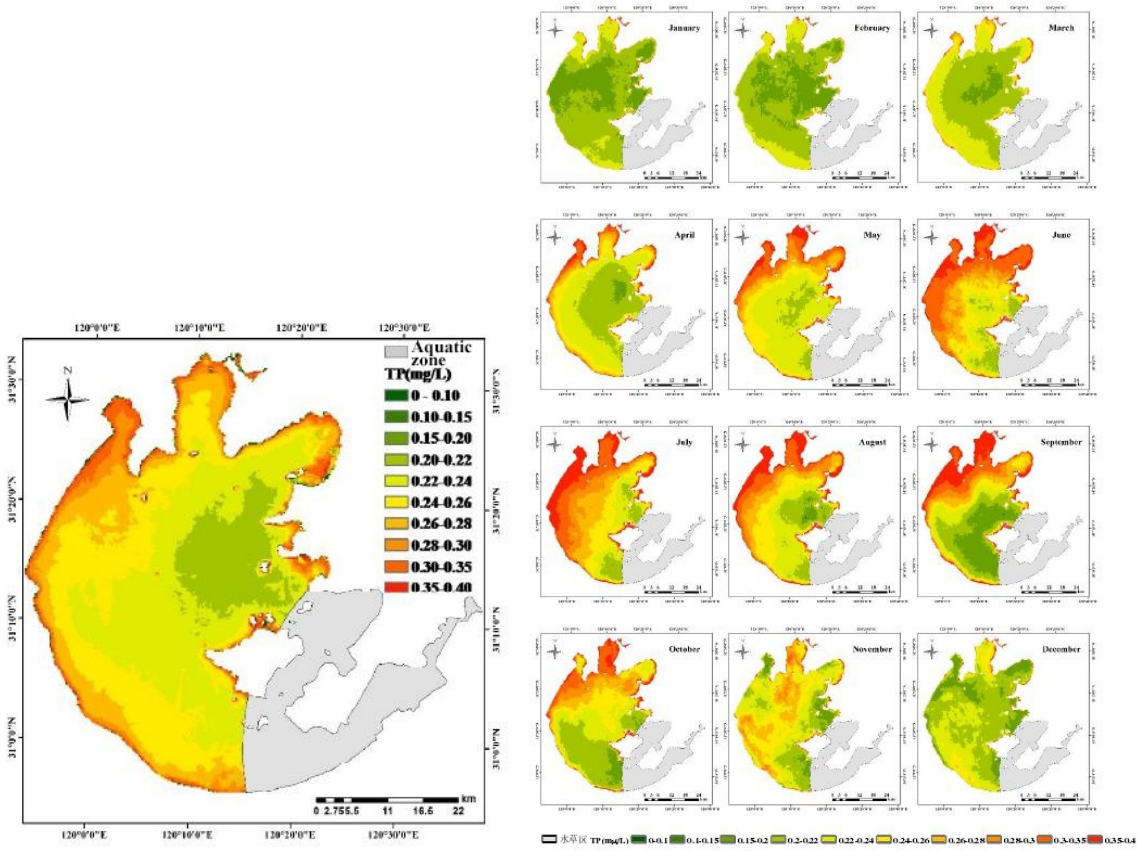

Fig. 34 (a) Spatial distribution of total phosphorus concentration in Taihu Lake. The spatial difference of total phosphorus concentration was obvious, with the highest value of 0.38mg/L and the lowest value of 0.06mg/L. (b) Monthly variation of total phosphorus concentration in different lakes.

The lake area also generally reaches its maximum phosphorus concentration between June and September. The total phosphorus concentration in Zhushan Bay, Meiliang Bay and the west bank of Taihu Lake was higher than the mean value of the whole lake from March to October of the year, and was significantly higher than that in the rest of Taihu Lake. The total phosphorus concentration in Gonghu Bay was higher than that in the whole lake only in June, and the total phosphorus concentration in the south bank of Taihu Lake and Great Taihu Lake was relatively low throughout the year.

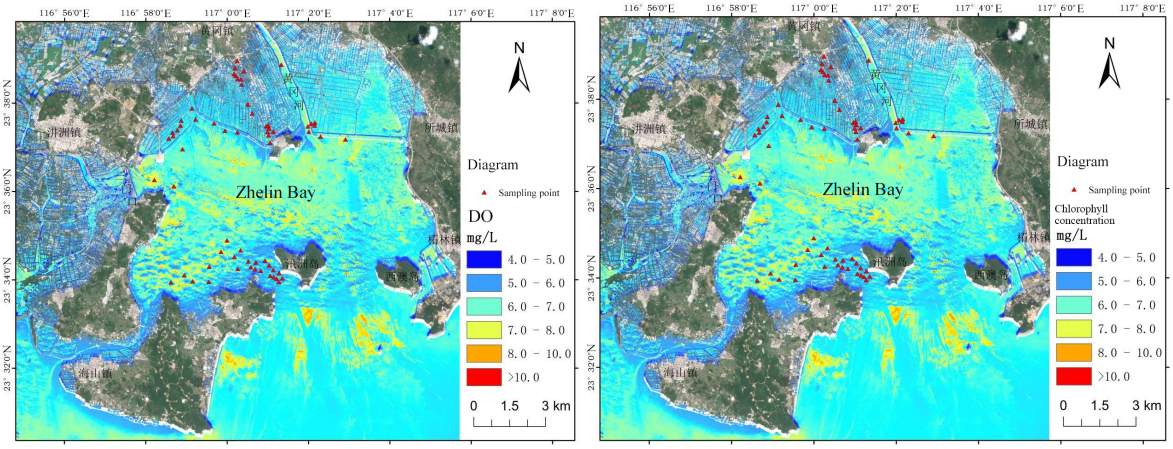

Figure 35 The distribution of dissolved oxygen and chlorophyll concentration in Zhelin Bay, eastern Guangdong, taken by hyperspectral